Nanotechnology **18** (2007) 205305 (7pp) doi:10.1088/0957-4484/18/20/205305

Hierarchical magnetic assembly of nanowires

Carlos M Hangarter[1], Youngwoo Rheem[1], Bongyoung Yoo[1], Eui-Hyeok Yang[2] and Nosang V Myung[1]

[1] Department of Chemical and Environmental Engineering and Center for Nanoscale Science and Engineering, University of California-Riverside, Riverside, CA 92521, USA
[2] Department of Mechanical Engineering, Stevens Institute of Technology, Hoboken, NJ 07030, USA

E-mail: myung@engr.ucr.edu

Received 12 January 2007, in final form 9 March 2007
Published 23 April 2007
Online at stacks.iop.org/Nano/18/205305

Abstract
Magnetic alignment is reported as a facile technique for assembling nanowires into hierarchical structures. Cross junction and T junction nanowire networks are demonstrated using a sequential alignment technique on unpatterned substrates and predefined lithographically patterned ferromagnetic electrodes. The formation of T junctions prevails as nanowires from the first alignment behave as ferromagnetic electrodes under the external magnetic field of the second alignment. The presence of prefabricated ferromagnetic electrodes dominates dipole interactions of localized nanowires for preferential alignment. Application of a magnetic field from a cylindrical coaxial magnet has also been utilized to form radially aligned nanowires. The magnetic field of the coaxial cylindrical magnet produced a dense, concentric nanowire configuration at the centre of the magnetic field as a consequence of the radial field gradient, and sparse nanowire arrangements in the peripheral field, which were utilized as interconnects with a concentric electrode design.

(Some figures in this article are in colour only in the electronic version)

1. Introduction

One-dimensional (1D) nanostructures, including nanowires, nanobelts, and nanorods, are the focus of many research groups because of their potential applications in electronics, spintronics, optoelectronics, photonics and sensors. These entities are building blocks for the bottom-up approach, being rigorously developed as the successor to top-down technologies. The small size and high aspect ratio of these nanostructures are amenable to high density devices, and the diameter of these entities falls within a quantum regime in which properties can be tailored by controlling diameter [1].

While research efforts have characterized these 1D nanostructures using costly and time-consuming techniques, nanomanufacturing has been stunted by controllable integration into existing technologies. Commercialization of nanowire and other 1D nanostructure based devices requires the ability to spatially manipulate and interface these structures with micro-and macro-components in a cost-effective manner. Several methods have demonstrated significant strides in this area (e.g. electric alignment [2], Langmiur–Blodgett [3] (LB), microfluidics [4] and optical manipulation [5]). However, each is met with its own limitations. Many of these techniques require post-alignment contact, which may increase the cost and complexity, necessitating procedures for locating structures followed by contact, usually via electron-beam lithography. Magnetic alignment circumvents these steps by aligning nanowires to predefined lithographically patterned ferromagnetic electrodes. Moreover, magnetic alignment is an innocuous tool for nanowire manipulation and integration, bypassing surface functionalization steps [3, 6] and potentially damaging electric potentials [7].

Here we report the use of magnetic assembly as a facile technique for aligning and positioning nanowires for complex structures, a critical step for realizing nanowire devices. Hierarchy provides the functional complexity to create useful devices from a small set of building blocks. The most basic operations can be observed with simple

nanowire heterojunctions of p- and n-type semiconductors to convert energy [8] or perform single-bit logic and memory functions [9]. In this regard, magnetic alignment is an appealing approach, relying on an intrinsic energy source, capable of aligning thousands of nanowires in a single step. With the appropriate applied external magnetic field, this method can facilitate two-step nanowire junctions or single-step radial alignment. In sequential alignments, deposited nanowires behave as ferromagnetic electrodes for subsequent nanowire alignments. Pre-fabricated ferromagnetic microelectrodes provide an additional degree of control, dominating dipole interactions among nanowires, for site-specific assembly.

2. Experimental procedure

Ferromagnetic nanowires (i.e. nickel, cobalt, permalloy ($Ni_{80}Fe_{20}$)) were synthesized by a template-directed electrodeposition method, being generally described by electrodeposition of material into a nanoporous scaffold [10, 11]. The templates used for these experiments were commercially available alumina membranes (Whatman, Inc. Anodisk 13) with a nominal pore size of 200 nm. One side of the templates was sputtered with gold using an Emitech K550 tabletop sputter coater to form a seed layer. The working electrode was constructed from a glass slide for mechanical support and double-sided copper tape (3M, 1182a) used as an electrical conductive path and an adhesive to secure the template against the slide. The copper tape and edges of the template were electrically masked using a red mylar insulting tape and Miccrostop, a dielectric surface coating.

The electrochemical cell for nickel electrodeposition was a 250 ml glass jar with 200 ml of the electrolyte exposed to ambient conditions and agitation with a 1″ stir bar at 300 rpm. The nickel nanowires were electrodeposited potentiostatically at −0.96 V using a three-electrode configuration: the aforementioned working electrode, a nickel counter electrode and a saturated calomel electrode (SCE) as a reference electrode. The nickel plating solution consisted of 1.61 M nickel sulfamate, 0.34 M nickel chloride and 0.36 M boric acid at pH of 2.96. Boric acid was added as a pH buffer. Deposition rate of nickel was approximately 11 μm h^{-1}. All solutions were made with ultra-pure water. Cobalt was also electrodeposited potentiostatically using the same cell with a three-electrode configuration. The cobalt plating solution consisted of 1 M cobalt sulfate, 0.81 M boric acid, and 0.12 M sodium chloride. The applied deposition potential was fixed at −1.00 V versus SCE. A platinum coated titanium stripe was used as a counter electrode. Deposition rate of cobalt was approximately 45 μm h^{-1}. The permalloy plating solution consisted of 0.2 M $NiCl_2$, 0.05 M $FeCl_2$, 0.7 NaCl, 0.4 H_3BO_3, 0.004 M sodium saccharin and 0.05 M L-ascorbic acid with a pH of 3 [12]. L-ascorbic acid was added to prevent the oxidation of ferrous ions to ferric ions. Saccharin was added to reduce the residual stress. Similar to cobalt electrodeposition, a platinum coated titanium strip was used as a counter electrode. Permalloy was deposited galvanostatically at 5 mA cm^{-2} with a deposition rate of approximately 1.5 μm h^{-1}. Deposition of the nanowires was controlled using an EG&G Princeton Applied Research VMP-2 Galvanostat/Potentiostat. Deposition time was adjusted to control the length of the nanowires.

A razor blade was used to remove the copper tape and mylar tape surrounding the template. The remaining tape and template were removed from the slide by immersing in acetone for 4 h. The template was then washed in acetone under sonication for 4 min to remove adhesive residue followed by detergent under sonication for 4 min, and rinsed in ultra-pure water. The gold seed layer was mechanically removed from the nanowire embedded template by hand polishing on 600 grit SiC polishing paper in water. After removal of the seed layer the template was dissolved in 1 M NaOH at room temperature for 2 h. The remaining nanowires were separated from solution by centrifuging at 5000 rpm and washed three times in ultra-pure water followed by isopropanol, which was the solution for the final nanowire suspension. Good dispersion of nanowires in solution was achieved by intermittent low power sonic agitation for several seconds.

The patterned gold electrodes for linear and radial alignments, shown in figures 3 and 7, were micro-fabricated by standard lift-off lithography, using a chromium adhesion layer. The microbands of the electrode configuration for radial alignment were electroplated with nickel using a current density of 5 mA cm^{-2} for 30 s with the same nickel electrolyte described above in a two-electrode configuration. The substrates were electrically contacted with double-sided copper tape and silver paint.

Cross- and T junction magnetic alignment was conducted on glass slides and patterned silicon substrates by placing the samples between two ceramic magnets. The magnetic field strength (i.e. 280, 760 and 1240 Gauss) was controlled by adjusting the gap distance between magnets. Radial alignments were conducted on glass substrates and patterned silicon substrates with a coaxial cylindrical magnet with magnetic field strengths of 800 G. The nanowire suspension was manually pipetted with a Brinkmann Eppendorf 2100 series 10 μl pipetter and dispensed in a 2–4 μl volumes on substrates placed between two permanent magnets for linear alignments and on top of the coaxial cylindrical magnet for radial alignments. Magnetic fields were measured using a F W Bell model 9500 Gaussmeter. Optical images were taken with a Hirox K-3000 digital microscope. Micrographs were taken using a Philip XL30-FEG scanning electron microscope (SEM).

3. Results and discussion

Magnetic alignment has been previously shown to exhibit excellent control over directionality and placement, by controlling external applied magnetic field strength in conjunction with electrode geometry, for individually addressable nanowires and nanowire arrays [13–16]. The dipoles of ferromagnetic nanowires in solution only align along the easy axis as a result of the shape anisotropy [17]. In addition, the high aspect ratio of these nanowires, $k = 50$, and hence small demagnetization factor, ultimately enhance susceptibility and remanence [17, 18]. Alignment parallel to the applied magnetic field results from the magnetic moment produced in suspended nanowires,

$$L = mlH \sin\theta \tag{1}$$

where m is the pole strength, l is the wire length and H is the applied magnetic field [18], which is of the magnitude of 10^{-14} N m. The chaining of ferromagnetic nanowires, described by Searson and co-workers as a function of inter-nanowire distance, viscous drag, nanowire dimensions and magnetization, is a consequence of nanowire–nanowire magnetic dipole interactions that dominate in solution [19].

The complete force balance for nanowire alignment under an applied magnetic field will also include terms for gravity,

$$F_{\text{total}} = F_{\text{magnetic}} + F_{\text{drag}} + F_{\text{buoyancy}}. \tag{2}$$

The buoyancy force,

$$F_{\text{buoyancy}} = (\rho - \rho_{\text{fl}})Vg \tag{3}$$

as described by density of the nanowire, ρ, the fluid density, ρ_{fl}, nanowire volume, and gravity, is shown as a function of nanowire length in figure 1(A) inset. The magnetic force exerted on a nanowire can be determined from Maxwell's equation for dipole interactions, which for a single nanowire suspended in solution can be described by the sum of interactions for all magnetic poles in the vicinity of the wire, including other nanowires and ferromagnetic electrodes, for each end of the wire. The total force on a nanowire with poles m_1 and m_2, resulting from neighbouring poles m_i and m_j, separated by a distance of r_i and r_j, respectively, can be described as

$$F = \sum_i \frac{m_1 m_i}{4\pi\mu_0 r_i^2} + \sum_j \frac{m_2 m_j}{4\pi\mu_0 r_j^2}. \tag{4}$$

Here μ_0 is the permeability of free space. The forces exerted on a single nanowire by another nanowire and by an electrode are shown as a function of separation distance in figure 1(A). For the nanowire–electrode interaction the superposition integral was used to account for the electrode edge geometry with respect to the nanowire point charge. Lastly the drag force can be calculated using the Stokes equation for drag in low Reynolds number systems,

$$F_{\text{drag}} = 6\pi\mu RU \tag{5}$$

where μ is the viscosity, U is the velocity and R is the translational tensor that can be interpreted as an equivalent radius [20]. Thus for a cylinder of length, a and diameter, b, the translation parallel to each has been described by Brenner [21] as:

$$R_a = \frac{2/3a}{\ln(2a/b) - 0.81} \tag{6}$$

$$R_b = \frac{4/3a}{\ln(2a/b) + 0.19}. \tag{7}$$

By further assuming drag is the only opposing force to gravity in the perpendicular direction, and the only opposing force to magnetic forces, the resulting velocities parallel and perpendicular to the cylindrical axis can be determined as a function of force, figure 1(B).

These suspended nanowires and nanowire chains will eventually partition to the substrate surface as the solution evaporates. However, because isopropanol is used to suspend nanowires in these experiments, chaining events also occur as a result of evaporation-induced deposition of the nanowires

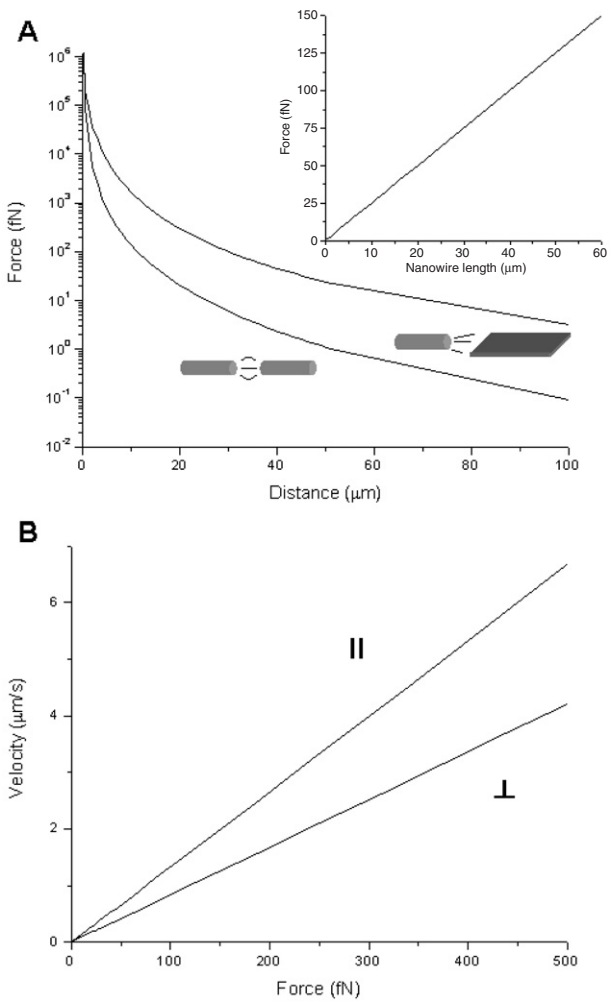

Figure 1. (A) Force due to magnetic dipole interactions for two collinear nickel nanowires with lengths of 10 μm and for a 10 μm nickel nanowire and a 10 μm wide nickel plated microband electrode. Inset is buoyancy force of 200 nm nickel nanowires as a function of nanowire length. (B) Velocity as a function of drag force parallel and perpendicular to the nanowire axis.

on the substrate as the solvent dries in under 60 s. The high contact angle of this solvent results in substrate coverage of approximately 1 cm^2 and rapid evaporation as a thin film. Although the surface tension,

$$\gamma = F/l \tag{8}$$

can create a torque on these nanowires, an order of magnitude greater than the applied magnetic field, 10^{-13} N m, the directionality is not significantly disrupted by the advancing interface. This is because deposited nanowires are subject to van der Waals forces and electrostatic forces that prevent their movement and free moving nanowires cannot experience a significant torque from surface tension forces as they are not anchored and subject to the magnetic moment during and immediately after the surface tension forces, allowing for final alignment.

This control over directionality is particularly crucial for functional nanowire assemblage. Sequential alignments have been demonstrated with microfluidics [4], and LB [3]

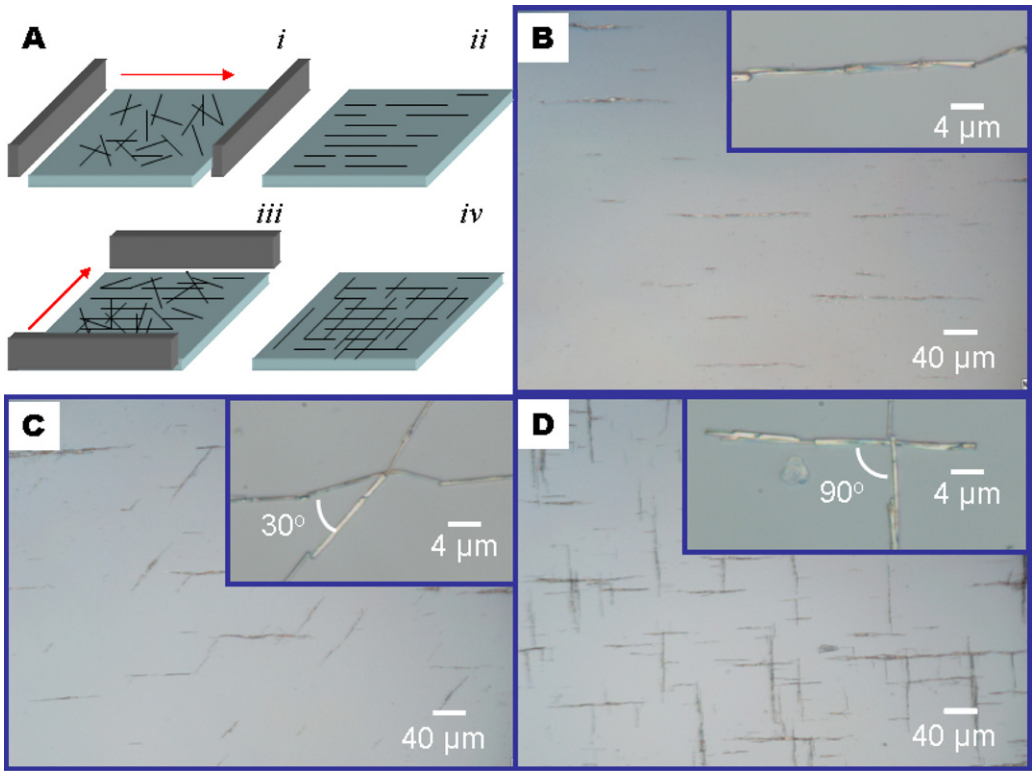

Figure 2. (A) Schematic illustrating the two-step process for sequential alignment: (i) dispensing the nanowire suspension in an external magnetic field (arrow), (ii) alignment of the nanowires, (iii) dispensing additional nanowire suspension under an opposing magnetic field (iv) and the second alignment of the suspended nanowires. (B) The alignment of the nanowires in a single direction using a 760 G field. (C) A two-step alignment with the substrate shift of 90° between dispensing, indicated by the inset. (D) A two-step alignment with a substrate shift of 30° between alignments, indicated by the inset.

as a proposed technique for creating hierarchical structures. Figure 2(A) highlights the procedure of this method with magnetic alignment on an unpatterned substrate with the first alignment shown in figure 2(B) and second alignments in figures 2(C) and (D). The insets in figures 2(C) and (D) indicate the degree of control with magnetic alignment, forming junctions from 30° to 90° with an externally applied magnetic field. The nanowires aligned in the first step were held in place by electrostatic forces and van der Waals forces, which are strong enough to withstand hydrodynamic forces of subsequent drops and opposing magnetic moments of subsequent alignments.

A large enough applied magnetic field can polarize deposited nanowires along their hard axis, perpendicular to their cylindrical axis [17], allowing the nanowires to behave as ferromagnetic electrodes, promoting the formation of T junctions, figure 3(A), in subsequent alignments. Weaker applied magnetic fields (e.g. 200 G) are not sufficient to magnetize nanowires from the first alignment completely perpendicular to their axis. Instead these wires experience a partial rotation in their domains with the ends still significantly magnetized because of their high shape anisotropy but with a demagnetization field slightly rotated to compensate for the applied magnet field. Slight angle offsets between the nanowire and applied magnetic field will contribute to this phenomenon and decreasing the angle between these alignments will further enhance this effect. As a consequence of these rotated domains, nanowires in second alignments

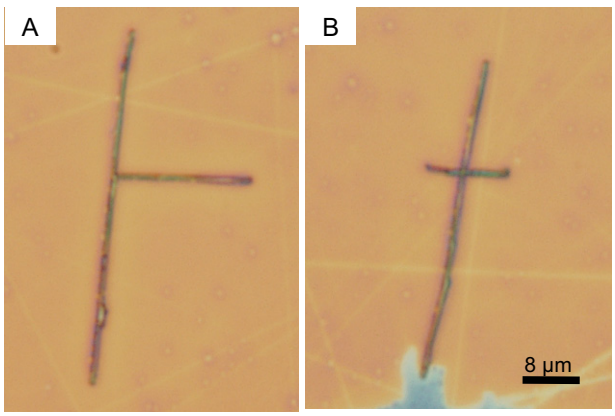

Figure 3. Optical images of 200 nm nanowire junctions. A T junction of a nickel (horizontal) and permalloy (vertical) nanowires and a cross junction with a permalloy (vertical) nanowire positioned on top of a nickel (horizontal) nanowire are shown in (A) and (B), respectively.

may form T junctions by positioning the second nanowire against the end of a previously aligned nanowire or by aligning end to end in an L configuration. A crossed nanowire junction (figure 3(B)), which occurs in smaller proportion, 12%, increases in number with the length of the nanowires as the dipoles of the deposited nanowire are separated by a greater distance.

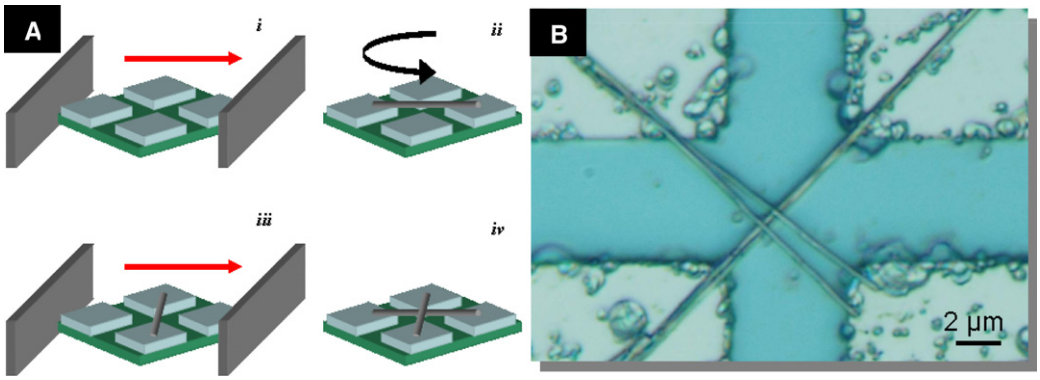

Figure 4. (A) The two-step alignment procedure with (i) alignment in a single direction, (ii) followed by a substrate shift, (iii) applying an external magnetic field in an opposing direction and (iv) the second alignment step. (B) A junction of crossing nickel nanowires on a ferromagnetic electrode.

Lateral aggregates which are apparent in figure 2(D) can be attributed to nonlinear magnetic interactions for sufficiently high dipole strengths and nanowire concentrations. These clusters are also influenced by nanowire concentration, rapid nanowire motion from a low viscosity fluid and large translational forces [18] that result from strong applied magnetic fields. The dominating forces in this system are magnetic forces and viscous drag [19]. For a low viscosity fluid, such as ispropanol, nanowires have little drag force to prevent them from reaching speeds comparable to their lengths. Stronger permanent magnets have larger field gradients, which produce more significant translational forces [18]:

$$F_x = ml\partial H/\partial x. \tag{9}$$

This force can create large nanowire concentration gradients, resulting in undesirable accumulation and aggregate formation at the droplet edge adjacent to the fixed magnets. Evaporation-induced inter-nanowire distance reduction may also have detrimental effects on magnetic alignment as the nanowires in these experiments are suspended in isopropanol, which evaporates in a matter of seconds for microlitre volumes.

On patterned substrates, the ferromagnetic electrodes behave as micromagnets creating dominant dipole interactions with nanowires for alignment adjacent to electrodes, as shown in figure 1(A). Introduction of a localized magnetic field with ferromagnetic electrodes disrupts weaker translational forces and generates a net force on nanowires resulting from the ferromagnetic electrodes and, to a less extent, localized nanowires. These interactions can be utilized to fabricate nanowire cross junctions on predefined electrodes by sequential alignment as shown in figure 4(B). The formation of ferromagnetic nanowire interconnects between two ferromagnetic electrodes can be viewed as a magnetic circuit in which nanowires preferentially align between the gap to lower the reluctance, because of its increased permeability with respect to the solution. Since the force between dipoles is proportion to the inverse square of the separation distance between them, it is still crucial to localize nanowires to the vicinity of the electrode for preferential alignment to occur. To achieve electrical contact several post-assembly techniques can be used to address nanowires on patterned and unpatterned substrates. These methods, demonstrated elsewhere, include nanoscale solder [13, 15, 22], annealing [16, 23] and lithography [4, 9].

A coaxial cylindrical magnet was utilized for radial alignment of ferromagnetic nanowires (figure 5(A)). Alignment trials revealed a dense ring in the middle of the substrate, with almost no nanowires within this ring and greater dispersion extending outside the ring. While control of nanowire suspension concentration was sufficient for outer-ring nanowire alignment, the centre of the ring was subject to singularities. The ring formation is a consequence of the radial field gradient generated by the core, drawing nanowires from solution towards the centre where the magnetic field is strongest [18]. The singularities in the centre occur in a small region directly in the centre of the core where the radial field gradient is diminished and an axial field gradient perpendicular to the surface dominates, resulting in no preferential alignment as the solution evaporates and no radial field gradient to draw nanowires further to the centre. Alignment defects in this region are also influenced by interaction with other nanowires. Chaining and aggregation was also less prevalent in radial arrangements when compared to linear alignments, and is due to an axial gradient that draws nanowires to the substrate, perpendicular to the surface. This field gradient creates more favourable alignment adjacent to the substrate standing on end as opposed to perpendicular chaining structures which are less stable. As the solution evaporates these nanowires, which are standing, lay down in a concentric fashion as directed by the radial field gradient. Chaining and defect structures that do form during radial alignments occur during this step as the solution evaporates, with magnetic interactions and strong surface tension forces that cause neighbouring nanowires to aggregate without the potential for recovery. In addition, almost no nanowires aligned over the nonmagnetic annulus. The field gradients draw the nanowires to the area of the substrate above the magnetic core and magnetic annulus as shown in figure 6.

Introduction of a circular ferromagnetic electrode did not mitigate the singularities or dense nanowire ring formation. However, the electrode configuration did demonstrate alignment success on the outskirts of the ring where nanowire placement was sparse. As depicted by the upper right inset for figure 7 the electrode for radial alignment consisted of a large, gold circular electrode surrounded by dozens of microbands oriented towards the centre of the circle.

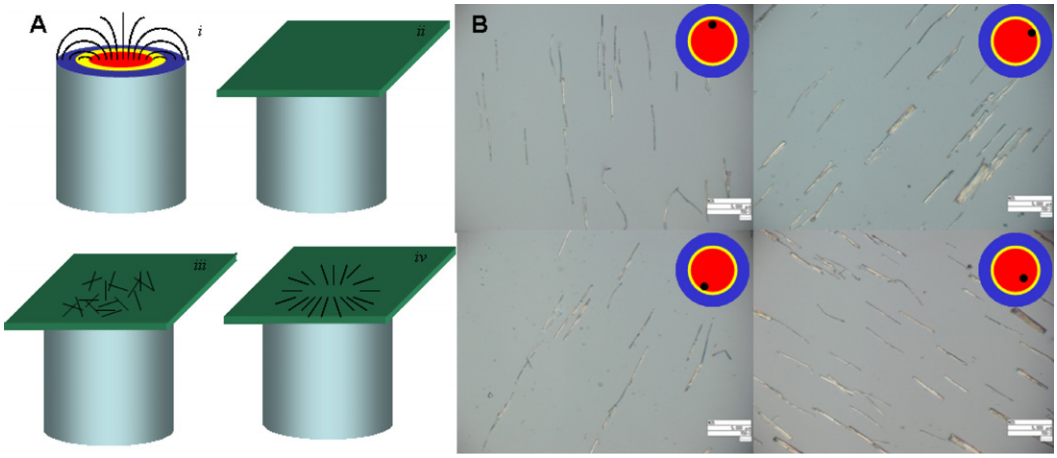

Figure 5. (A) Radial alignment consists of a (i) cylindrical coaxial magnetic, (ii) with a substrate placed on one end, (iii) for the nanowire suspension to be dispensed upon and (iv) aligned. The coaxial cylindrical magnet has a magnetic core (centre cylinder/red) and a magnetic annulus (outer annulus/blue) separated by a nonmagnetic annulus (inner annulus/yellow). (B) An optical image of radially aligned nickel nanowires on an unpatterned substrate using an 800 G cylindrical coaxial magnet. The insets indicate the position (black dot) over the coaxial magnet from which these alignments were taken from.

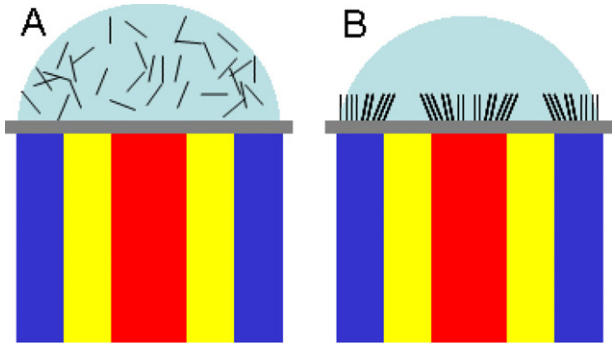

Figure 6. Cross-sectional view of nanowire alignment in solution and cylindrical coaxial magnet. Field gradients cause (A) randomly ordered nanowires in solution to migrate to the surface, (B) aligning over the magnetic core (red) and magnetic annulus (blue) perpendicular to the substrate (grey) and parallel to applied fields.

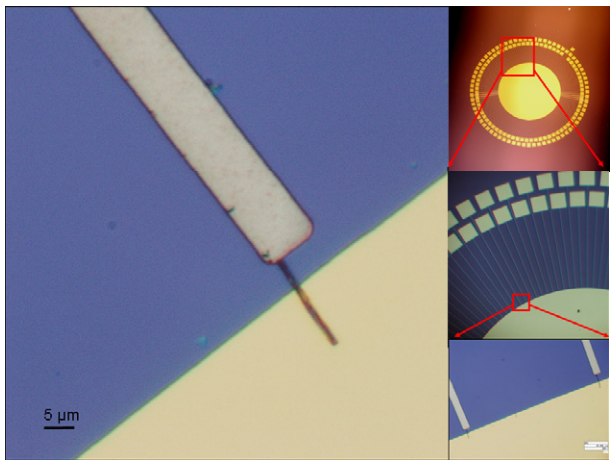

Figure 7. Optical image of a radially aligned nanowire interconnect. The inset is an optical image of the entire electrode configuration (upper right), a circular electrode surrounded by microbands concentrically directed towards the circular electrode, with an enlarged image for perspective and a further enlarged image to showing radially aligned flanking nanowires.

In this system only the fingers were electroplated with a ferromagnetic material for selective alignment of nanowires. Dispensing location of the nanowire solution droplet was critical for alignment with the circular electrodes. The electrode–nanowire separation distance must be sufficiently small for the force imposed by the magnetic fingers to prevent concentric nanowire migration caused by the radial field gradient,

$$F = ml\partial H/\partial r. \tag{10}$$

Dispensing 5 μl of the nanowire suspension in the middle of the circular electrode produced a dense ring formation as previously mentioned with no aligned nanowires as the electrode diameter overextended the diameter of the coaxial magnet. However, by dispensing the nanowire suspension directly over the electrode gaps several nanowire interconnects were produced (figure 7).

The localized magnetic field established by ferromagnetic electrodes disrupts the translational force and generates a net force on nanowires resulting from the ferromagnetic electrodes and local nanowires. The magnetic force on nanowires suspended in solution can be described by equation (1) as a sum of dipole interactions with all magnetic poles in the vicinity of the wire, including other nanowires and ferromagnetic electrodes. Each dipole interaction is proportional to the product between two poles and inversely proportional to the square of the distance between these two poles [18]. However, since the force is proportion to the inverse square of the separation distance between poles, it is still crucial to localize nanowires to the vicinity of the electrode for preferential positioning to occur. For these experiments localization was conducted by manually dispensing the nanowire suspension over the electrodes of interest. In most cases, preferential placement without aggregation was controlled by nanowire concentration.

4. Conclusion

Magnetic alignment was demonstrated as a method for fabricating hierarchical nanowire structures. Utilizing an unpatterned substrate and a weak applied magnetic field nanowires were sequentially arranged into networks comprised of cross junctions and T junctions. Nanowires aligned in the first step behaved as ferromagnetic electrodes for preferential formation of T junctions. The nanowire concentration and applied magnetic field were important parameters in reducing the lateral aggregation and droplet edge accumulation. We have also demonstrated the use of a cylindrical coaxial magnetic field for radial assembly of nanowire interconnects without registration. A dense nanowire ring formation over the centre of the coaxial cylindrical magnet is a consequence of the radial field gradient pulling nanowires from solution towards the centre of the field. The lack of nanowire chain formations was attributed to the axial field gradient, projected perpendicular to the substrate, aligning nanowires on end, in a vertical fashion, in solution. The substrated radial nanowire arrangements result from the radial field vector, which directs nanowires in a concentric fashion during evaporation-induced prostrate positioning. Radial alignment of nanowires to prefabricated electrodes, consisting of a circular common gold electrode and ferromagnetic microbands directed in a concentric fashion, demonstrated the importance of localizing nanowires in solution to the vicinity of the electrode gap to oppose the radial field gradient and facilitate preferential alignment.

Acknowledgment

This work is based on research sponsored by the Defense Microelectronic Activity (DMEA) under agreement number H94003-05-2-0505.

The United States government is authorized to reproduce and distribute reprints for government purposes, not withstanding any copyright notation thereon.

References

[1] Yu H, Li J B, Loomis R A, Wang L W and Buhro W E 2003 Two-versus three-dimensional quantum confinement in indium phosphide wires and dots *Nat. Mater.* **2** 517–20

[2] Smith P A *et al* 2000 Electric-field assisted assembly and alignment of metallic nanowires *Appl. Phys. Lett.* **77** 1399–401

[3] Whang D, Jin S, Wu Y and Lieber C M 2003 Large-scale hierarchical organization of nanowire arrays for integrated nanosystems *Nano Lett.* **3** 1255–9

[4] Huang Y, Duan X F, Wei Q Q and Lieber C M 2001 Directed assembly of one-dimensional nanostructures into functional networks *Science* **291** 630–3

[5] Pauzauskie P J, Radenovic A, Trepagnier E, Shroff H, Yang P D and Liphardt J 2006 Optical trapping and integration of semiconductor nanowire assemblies in water *Nat. Mater.* **5** 97–101

[6] Tao A *et al* 2003 Langmuir–Blodgett silver nanowire monolayers for molecular sensing using surface-enhanced Raman spectroscopy *Nano Lett.* **3** 1229–33

[7] Lao C S *et al* 2006 ZnO nanobelt/nanowire Schottky diodes formed by dielectrophoresis alignment across Au electrodes *Nano Lett.* **6** 263–6

[8] Huang Y, Duan X F and Lieber C M 2005 Nanowires for integrated multicolor nanophotonics *Small* **1** 142–7

[9] Huang Y, Duan X F, Cui Y, Lauhon L J, Kim K H and Lieber C M 2001 Logic gates and computation from assembled nanowire building blocks *Science* **294** 1313–7

[10] Martin C R 1994 Nanomaterials—a membrane-based synthetic approach *Science* **266** 1961–6

[11] Martin C R 1995 Template synthesis of electronically conductive polymer nanostructures *Acc. Chem. Res.* **28** 61–8

[12] Myung N V and Nobe K 2001 Electrodeposited iron group thin-film alloys—structure-property relationships *J. Electrochem. Soc.* **148** C136–44

[13] Ye H K, Gu Z Y, Yu T and Gracias D H 2006 Integrating nanowires with substrates using directed assembly and nanoscale soldering *IEEE Trans. Nanotechnol.* **5** 62–6

[14] Bentley A K, Trethewey J S, Ellis A B and Crone W C 2004 Magnetic manipulation of copper–tin nanowires capped with nickel ends *Nano Lett.* **4** 487–90

[15] Hangarter C M and Myung N V 2005 Magnetic alignment of nanowires *Chem. Mater.* **17** 1320–4

[16] Yoo B Y, Rheem Y W, Beyermann W P and Myung N V 2006 Magnetically assembled 30 nm diameter nickel nanowire with ferromagnetic electrodes *Nanotechnology* **17** 2512–7

[17] Sun L, Hao Y, Chien C L and Searson P C 2005 Tuning the properties of magnetic nanowires *IBM J. Res. Dev.* **49** 79–102

[18] Chikazumi So and Graham C D 1997 *Physics of Ferromagnetism* 2nd edn (New York: Oxford University Press)

[19] Tanase M *et al* 2001 Magnetic alignment of fluorescent nanowires *Nano Lett.* **1** 155–8

[20] Probstein R F 2003 *Physicochemical Hydrodynamics an Introduction* (Hoboken: Wiley)

[21] Brenner H 1974 Rheology of a dilute suspension of axisymmetric brownian particles *Int. J. Multiphase Flow* **1** 195–341

[22] Ye H, Gu Z, Yu T, Bernfeld A, Leong T and Gracias D H 2005 Forming low resistance nano-scale contacts using solder reflow *5th IEEE Conf. on Nanotechnology 2005 (Nagoya, Japan, July 2005)* pp 561–4

[23] Rheem Y, Yoo B Y, Beyermann W P and Myung N V 2007 Magnetotransport studies of a single nickel nanowire *Nanotechnology* **18** 15202